

Improved Performance of Colloidal CdSe Quantum Dot-Sensitized Solar Cells by Hybrid Passivation

Jing Huang,[†] Bo Xu,[‡] Chunze Yuan,[†] Hong Chen,[§] Junliang Sun,[§] Licheng Sun,^{*,‡} and Hans Ågren^{*,†}

[†]Department of Theoretical Chemistry & Biology, School of Biotechnology, Royal Institute of Technology (KTH), 106 91 Stockholm, Sweden

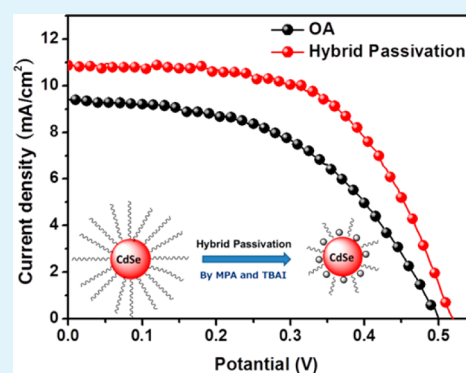
[‡]Organic Chemistry, Centre of Molecular Devices, Department of Chemistry, School of Chemical Science and Engineering, Royal Institute of Technology (KTH), 100 44 Stockholm, Sweden

[§]Berzelii Centre EXSELENT on Porous Materials, Department of Materials and Environmental Chemistry, Stockholm University, 106 91 Stockholm, Sweden

Supporting Information

ABSTRACT: A hybrid passivation strategy is employed to modify the surface of colloidal CdSe quantum dots (QDs) for quantum dot-sensitized solar cells (QDSCs), by using mercaptopropionic acid (MPA) and iodide anions through a ligand exchange reaction in solution. This is found to be an effective way to improve the performance of QDSCs based on colloidal QDs. The results show that MPA can increase the coverage of the QDs on TiO₂ electrodes and facilitate the hole extraction from the photooxidized QDs, and simultaneously, that the iodide anions can remedy the surface defects of the CdSe QDs and thus reduce the recombination loss in the device. This hybrid passivation treatment leads to a significant enhancement of the power conversion efficiency of the QDSCs by 41%. Furthermore, an optimal ratio of iodide ions to MPA was determined for favorable hybrid passivation; results show that excessive iodine anions are detrimental to the loading of the QDs. This study demonstrates that the improvement in QDSC performance can be realized by using a combination of different functional ligands to passivate the QDs, and that ligand exchange in solution can be an effective approach to introduce different ligands.

KEYWORDS: quantum dot-sensitized solar cells, colloidal quantum dots, hybrid passivation, solution process



INTRODUCTION

Quantum dots (QDs) have commonly been considered as promising candidates for the third-generation solar cells, owing to their broad and tunable light absorption, high extinction coefficient and low-cost solution-processed preparation.^{1–6} Accordingly, solar cells based on QDs have shown great progress in recent years; for example, the power conversion efficiency (PEC) for solid state depleted heterojunction cells with colloidal QDs has reached 8.5%,^{7,8} and the efficiency of quantum dot-sensitized solar cells (QDSCs) has approached 7%.^{9–11} Therefore, QD solar cells have been regarded as the next important step in photovoltaics.¹² Employing QDs as an alternative to organic dyes to construct QDSCs can not only improve the stability of the solar cells due to the inorganic nature of the QDs but also boost the theoretical PEC up to 44%,^{5,13} resulting from the desirable light harvesting and the potential of multiexciton generation (MEG).^{14,15}

To date, there are two main approaches that have been employed to deposit QDs onto wide bandgap nanostructured metal oxide (TiO₂, ZnO and SnO₂) electrodes, in situ and ex situ. In general, high coverage can be obtained from the in situ methods such as successive ionic layer adsorption and reaction

(SILAR) and chemical bath deposition (CBD),¹⁶ which usually present a high photocurrent and a desirable PEC.^{10,17} However, these methods allow little control over the size and shape of the deposited QDs, and the stability of the devices made by these methods still needs to be improved. For the ex situ approach, colloidal QDs are presynthesized, followed by deposition onto the photoelectrodes. Comparing with SILAR-deposited QDs, colloidal QDs can have several advantages benefiting from the controllable synthesis pathway, from which the size, shape, composition and surface property of the QDs could be optimized, as well as the improved crystallinity and stability.¹⁸ In addition, many studies have shown that multiple exciton generation can be observed from nearly monodispersed colloidal QDs, which could be attributed to the high quality of these nanostructures.^{14,19} So far, more and more QDSCs with a high PEC and long lifetime have been developed by using colloidal QDs. For instance, Jin et al. employed colloidal CdTe/CdSe QDs in QDSCs to achieve the PEC of 6.76%,⁹ and

Received: July 11, 2014

Accepted: October 13, 2014

Published: October 13, 2014

Pan et al. developed high-performance QDSCs by using low-cost and low-toxicity CuInS₂/ZnS colloidal QDs.¹¹

Despite of the huge potential of colloidal QDs, the efficiency of QDSCs still cannot be comparable to that of dye-sensitized solar cells (DSCs). To the best of our knowledge, the major factors limiting the performance of QDSCs are the low coverage of colloidal QDs on the photoanodes,²⁰ caused by the native long hydrocarbon chains commonly used as capping ligands around the QDs, and the charge recombination occurring at the QDs surface traps due to imperfect surface atomic termination.²¹ Surface modification could be an effective way to address these two problems, because some chemical properties, such as the solubility in different solvents, the surface states, and the functional behavior for coupling the nanoparticles with other molecules, are dominated by the ligands of the QDs.^{22,23} The works by Zhong's group have shown that ligand exchange by bifunctional mercaptopropionic acid (MPA) can significantly increase the loading amount of QDs,^{9,24,25} where the -SH groups bind to the metal atoms of the QDs and the -COOH groups anchor to the TiO₂ electrodes. However, the original trap states on the surface of the QDs, which can cause serious recombination of charge carriers, cannot be effectively reduced by ligand exchange with MPA. Recently, Sargent et al. have established an atomic ligand strategy by using monovalent halide anions to passivate the surface defects of colloidal PbS QDs for heterojunction quantum dot solar cells.^{26,27} Through systematic studies, it was uncovered that the atomic ligand passivation can remedy the problem of the trap states deep within the bandgap, contributing to superior charge carrier diffusion in the quantum dot films, and resulting in improved photovoltaic performance.^{7,28} Furthermore, they developed a hybrid passivation scheme for PbS quantum dot films by introducing halide anions after MPA treatment to further increase the efficiency of solar cells.²⁹

To improve the performance of QDSCs, we introduce in this study a hybrid passivation strategy to colloidal CdSe QDs by employing MPA to increase the loading amount of QDs and importing iodide anions through tetrabutylammonium iodide (TBAI) to decrease the recombination loss in the device. Differently from the published hybrid passivation performed on quantum dot films, the passivation in this work was carried out by a solution process through a ligand exchange reaction, which hypothetically offers the passivants a higher degree of accessibility to the surface of the QDs, and maximizes the opportunity to modify the surface states.²⁸ Passivation only with MPA or iodide anions was performed as comparison, and original oleic acid (OA) capped CdSe QDs were employed as reference. UV-vis spectra indeed demonstrated that hybrid passivation can make CdSe QDs achieve much higher loading on TiO₂ electrodes, resulting in an increased photocurrent. The recombination can be significantly suppressed, owing to the enhanced hole extraction by MPA and the reduced surface traps by iodine atoms, thus boosting the fill factor value of the QDSCs. The effect of different amount of iodide anions in hybrid passivation was also investigated, showing that excessive iodide anions do not favor the deposition of QDs on TiO₂ electrodes, leading to inferior performance of the devices.

EXPERIMENTAL DETAILS

Materials. Cadmium oxide (CdO, 99.998%), tri-*n*-octylphosphine (TOP, 90%) and oleic acid (OA, 90%) were purchased from Alfa Aesar; selenium powder (99%), 3-mercaptopropionic acid (3-MPA,

>99%) and tetrabutylammonium iodide (TBAI, 98%) were purchased from Sigma-Aldrich, paraffin was from J.T Baker. All chemicals were used as received.

Synthesis of Colloidal CdSe QDs. A literature method was adopted to synthesize CdSe QDs with slight modifications.³⁰ Briefly, 0.5 mL of a Se precursor solution (0.1 M), prepared by dissolving Se powder in TOP and paraffin (v/v, 1:3) at 60 °C under Ar atmosphere, was added to 5 mL of a Cd precursor solution (0.1 M), obtained by dissolving CdO in a mixed solution of OA and paraffin (v/v, 1:3) at 200 °C under Ar atmosphere, in a three-neck flask at room temperature. The mixture was then degassed at 110 °C for 10 min under vacuum, following by heated to 280 °C at a rate of 10 °C/min under Ar atmosphere. The reaction system stayed at 280 °C for 10 min before removing the heater and cooling to 60 °C. After synthesis, the nanocrystals were precipitated with methanol, and then washed by repeated resuspending in chloroform and precipitation with addition of methanol. For convenience, these as-prepared QDs are referred as OA-CdSe QDs.

Hybrid Passivation of Colloidal CdSe QDs. The passivation of QDs was achieved by a ligand exchange reaction. For hybrid passivation, the ligand solution was formed by adding TBAI aqueous solution (dissolving 10 mg TBAI in 100 μ L deionized water) into the MPA solution, which was prepared by dissolving 150 μ L of MPA into 0.5 mL of methanol, and then 40% NaOH was added to adjust the pH of the MPA solution to 12. Then the exchange reaction was performed by dropping the ligand solution into 5 mL of OA-CdSe QDs stock solution (5 mM, dispersing in chloroform solution) under strong stirring. After the solution was stirred for 40 min at room temperature, passivated QDs were collected and washed by water and acetone, and finally dispersed in deionized water. Passivation with MPA followed a similar procedure, except that the ligand solution was just MPA solution. CdSe QDs passivated only by iodide anions were prepared by adding 10 mg of TBAI to 5 mL of OA-CdSe QDs stock solution with stirring for 40 min at room temperature, followed by precipitation with methanol, and then dispersing in a chloroform solution.

Fabrication of QD-Sensitized Photoanodes. TiO₂ mesoporous electrodes with a light-scattering layer were prepared by a screen printing method on F-doped tin oxide (FTO) glass. A transparent layer with a thickness of 7 μ m and a 4 μ m scattering layer were made by commercial paste from Solaronix (Ti-Nanoxide T/SP for transparent layer, and Ti-Nanoxide R/SP for scattering layer), followed by annealing at 500 °C for 30 min. The area of TiO₂ layers was 0.25 cm². The sintered electrodes were post-treated by aqueous TiCl₄ solution (40 mM) at 70 °C for 40 min.

QD-sensitized photoanodes were obtained by directly pipetting 100 μ L of CdSe aqueous solution (0.017 M) onto TiO₂ electrodes. After the solution was left for 2 h in open air, the excess CdSe QDs was removed by rinsing with water. This procedure was repeated once to increase the loading amount of QDs. After the deposition was finished, the QD-sensitized TiO₂ electrodes were treated with two circles of ZnS by immersing the photoanodes into Zn(NO₃)₂ aqueous solution (0.1 M) and Na₂S aqueous solution (0.1 M) for 1 min/dip alternately.

Preparation of Cu₂S Counter Electrode. The counter electrodes were prepared by immersing polished brass foils into HCl (37%) solution at 80 °C for 10 min and washed by water, which was followed by sulfidation in the prepared polysulfide electrolyte solution.

Polysulfide Electrolyte and Assembling of Solar Cells. The polysulfide solution contained 2 M S, 2 M Na₂S and 0.2 M KCl in a methanol-water (v/v, 3/7) solution. The solar cell was constructed by assembling a QD-sensitized photoanode and a Cu₂S counter electrode using a Surlyn film (50 μ m). The polysulfide electrolyte solution was then injected by vacuum backfilling.

Characterization. Transition electron microscopy (TEM) images together with energy-dispersive X-ray spectra were obtained on a JEOL JEM-2100 microscope at 200 kV. The powder X-ray diffraction (XRD) pattern was collected from a X'Pert PANalytical PRO MRD using Cu K α radiation ($\lambda = 1.54056 \text{ \AA}$). UV-vis absorption spectra were recorded on Lambda 750 UV-vis spectrophotometer. All solution samples were measured in a 1 cm cell at room temperature. TiO₂ film with only transparent layer on FTO glass was used for

absorption measurement of QDs sensitized TiO₂ film. Fourier transform infrared spectroscopy (FTIR) was performed on a Biorad FTS 375 spectrometer. The sample for the measurement was prepared by mixing 1 mg of a QDs solid with 80 mg of KBr, following by pressing into a transparent film after grinding. Current–voltage characteristics were carried out by applying an external potential bias to the device while recording the generated photocurrent with a Keithley model 2400 digital source meter. The light source was a 300 W xenon lamp (Newport) calibrated with the light intensity to 100 mW·cm⁻² at AM 1.5 G solar light condition by a certified silicon solar cell (Fraunhofer ISE). IPCE spectra were operated on a computer-controlled setup comprised of a xenon lamp (Spectral Products ASB-XE-175), a monochromator (Spectral Products CM110) and a potentiostat (EG&G PAR 273). The setup was calibrated with a certified silicon solar cell (Fraunhofer ISE) prior to measurements. Impedance spectroscopy (IS) measurement was investigated with an impedance module from Autolab PGstat12 potentiostat.

■ RESULT AND DISCUSSION

Synthesis and Surface Passivation of QDs. CdSe QDs were synthesized via one-pot method with slight modifications from literature.³⁰ By using the air-stable noncoordinating solvent paraffin to slow down the reaction rate, a nearly monodispersed CdSe QDs product with a size range of 4.0 ± 0.3 nm was obtained, as shown in Figure 1. The XRD pattern

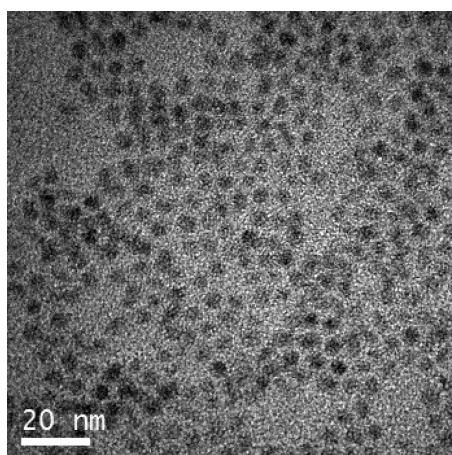


Figure 1. TEM image of the as-synthesized CdSe QDs.

(Figure S1, Supporting Information) shows that the as-synthesized QDs are cubic CdSe (PDF #19-0191), which is in agreement with the literature.³⁰ Because the molar ratio of

Cd precursor (Cd-OA)-to-Se precursor (Se-TOP) was 10/1, we suppose that the surface of CdSe QDs was rich of Cd atoms, and the excess of Cd atoms in the surface could facilitate the X-type ligand, iodide anions and MPA to exchange the original ligand of the QDs.³¹ Hybrid passivation was then performed to the as-synthesized CdSe QDs through a ligand exchange reaction. Specifically, the ligand solution was formed by adding TBAI aqueous solution into the basic MPA solution, the high pH value of which is very important for the deprotonation of -SH group in MPA to allow it to bind to Cd sites on the QDs surface.³² By dropping the ligand solution into the CdSe QDs chloroform solution, with constant stirring for 40 min at room temperature, the QDs transferred to the upper water phase from the underneath organic phase, which was indicated by the color of the upper phase turning red while the red color of organic phase disappeared. After washing, the hybrid passivated CdSe QDs dispersed in water easily, forming a clear bright red solution, and remained stable in aqueous media for more than one month, which may be attributed to the strong electrostatic repulsion between the negatively charged QDs after the ligand exchange reaction. The CdSe QDs passivated only by iodide anions were prepared by directly mixing of TBAI and OA-CdSe QDs in chloroform solution and stirring for 40 min at room temperature, whereas MPA passivated CdSe QDs were fabricated by a reaction between the MPA solution and the CdSe QDs chloroform solution.

Energy-dispersive X-ray spectroscopy (EDS) results of the different passivated CdSe QDs are presented in Figure 2a. Cu, Cr, Fe, Co and partial C signals in all spectra were contributed by TEM grids; Cd and Se peaks came from the QDs. There is no discernible peak of P in any spectrum, but C and O peaks can be detected from the as-synthesized QDs, indicating that the native ligand on the CdSe QDs was mainly OA, not TOP. After being passivated with iodide anions, I peaks appeared from the EDS spectrum; a S peak can be observed from the MPA passivated QDs. Both S and I signals can be detected from CdSe QDs with hybrid passivation, demonstrating that the QDs were successfully hybrid passivated by MPA and iodine anions. Fourier transform infrared (FTIR) spectra (Figure S2, Supporting Information) reveal that the oleate ligand (C–H vibration between 2800 and 3000 cm⁻¹) is significantly reduced by the MPA passivation and hybrid passivation, whereas ligand exchange with just iodide ions can only partially replace the long alkaline chain on the quantum dots. The combination of COO⁻ vibration conservation and C–H vibration reduction further proved that the original ligand

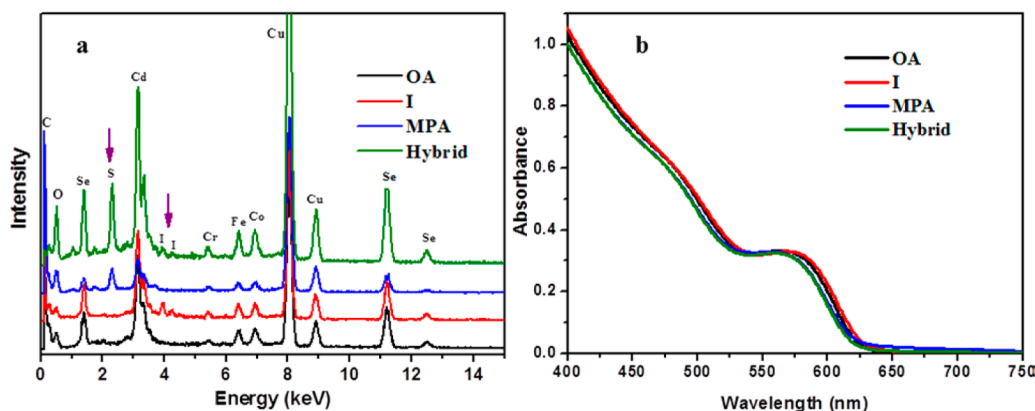


Figure 2. EDS spectra (a) and UV–vis absorption spectra (b) of CdSe QDs with different passivation in solution.

OA, which is capped on CdSe QDs, is substituted by MPA in the MPA passivation and hybrid passivation, and that the hybrid passivation can remove OA more completely. Figure 2b shows the UV-vis spectra of CdSe QDs after different passivation treatments. Comparing with the original CdSe QDs capped with OA, the absorption peak of the water-soluble hybrid passivated and MPA passivated CdSe QDs shows a slight blue shift, which may arise from the shorter ligand on the QDs and the polar solvent used in measurement.²² In contrast, the absorption peak of the atomic passivated CdSe QDs slightly move to longer wavelength. Through TEM images (Figure S3, Supporting Information), we find that the distance between CdSe QDs become shorter after ligand exchange by TBAI, decreasing the dispersibility of the QDs in chloroform and even causing partial aggregation of QDs, resulting in red-shifted absorption of atomic passivated CdSe QDs.

Deposition of QDs on TiO₂ Electrodes. CdSe QDs sensitized TiO₂ photoanodes were prepared by directly pipetting the CdSe QDs aqueous solution on TiO₂ films, and the QDs were kept for 2 h before being rinsed with water to remove unadsorbed QDs. This procedure was repeated once to increase the loading amount of the QDs. To evaluate the influence of hybrid passivation to the deposition efficiency of the CdSe QDs onto TiO₂ films, absorption spectra and corresponding photographs of different ligand capped CdSe-TiO₂ films are shown in Figure 3. It is apparent that the spectra

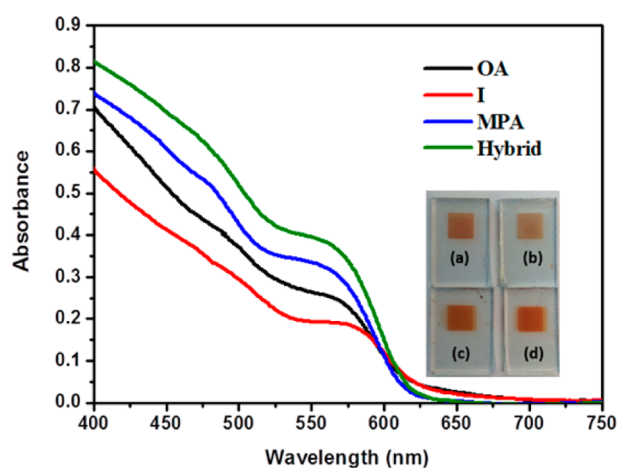


Figure 3. UV-vis absorption spectra of CdSe QDs-sensitized TiO₂ electrodes based on different surface passivation of QDs. Inset: photographs of (a) OA-CdSe/TiO₂ film, (b) iodide passivated-CdSe/TiO₂ film, (c) MPA passivated-CdSe/TiO₂ film, (d) hybrid passivated-CdSe/TiO₂ film.

of the QDs-sensitized TiO₂ films inherit the absorption characteristics of the colloidal CdSe QDs in solution. Comparing with the native ligand OA, passivation with MPA increases the absorbance of the CdSe-TiO₂ films, and hybrid passivation further improve the coverage of CdSe QDs on TiO₂ electrodes, which is also reflected by the most reddish color of the TiO₂ film sensitized with the hybrid passivated QDs. After the ligand exchange reaction, both the hybrid passivated and the MPA passivated CdSe QDs become water-soluble due to the capping ligand MPA, which can efficiently bind to TiO₂ electrode through the carboxyl group.³³ The high wettability and superior penetration capability of the water-soluble QDs also facilitate these two kinds of CdSe QDs to deposit on the hydrophilic TiO₂ electrodes to achieve high QDs-loading.²⁰ In

contrast, passivation only with iodide anions lower the absorbance of CdSe-TiO₂ films, and the first exciton peak shows slight red shift, consistent with the absorption of QDs in solution. This can be ascribed to the poor dispersibility of the atomic passivated CdSe QDs in chloroform. Therefore, the passivation containing MPA component can indeed increase the loading amount of QDs on TiO₂ electrodes. To further increase the coverage of colloidal QDs, the TiO₂ electrodes with large pore size can be employed as photoanode, which can allow more colloidal QDs to penetrate into the TiO₂ active layer and adsorb on the TiO₂ nanoparticles.

Device Performance. To investigate the effect of the hybrid passivation on the photoelectrical property of the CdSe QDs, we employed CdSe QDs with different treatments in a typical configuration of QDSCs, which is constructed by a TiO₂ photoanode, including a transparent layer and a scattering layer made by a screen-printing method, a Cu₂S counter electrode and a polysulfide methanol-water solution as the electrolyte. Two batches (three parallel cells in each batch) of every kind of passivated CdSe QDs based QDSCs were made for the photovoltaic measurement. The current density-voltage (*J*-*V*) characteristics of the QDSCs based on different kinds of passivated CdSe QDs were examined under the illumination of AM 1.5 G solar simulated light (100 mW·cm⁻²) with the mask of 0.25 cm², and the average performance is shown in Figure 4.

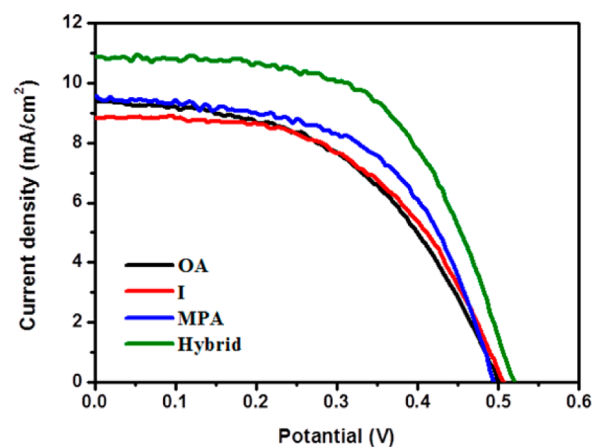


Figure 4. *J*-*V* curves of QDSCs based on CdSe QDs treated with different surface passivation.

The corresponding open circuit voltage (*V*_{oc}), short circuit current density (*J*_{sc}), fill factor (FF) value and overall power conversion efficiency (*η*) are summarized in Table 1. The statistical analysis of all the devices performance is shown in Figure S4 (Supporting Information). In comparison to the QDSCs assembling with native ligand OA capped CdSe QDs, we can see that the hybrid passivated CdSe-QDSCs exhibit significant improvement in the overall efficiency, which amounts to 3.31%, benefiting from higher *J*_{sc} (10.87 mA/

Table 1. Photovoltaic Parameters of QDSCs Based on CdSe QDs Treated with Different Surface Passivations

passivant	<i>V</i> _{oc} (V)	<i>J</i> _{sc} (mA/cm ²)	FF	<i>η</i> (%)
OA	0.500	9.42	0.496	2.34
I	0.505	8.82	0.535	2.38
MPA	0.495	9.60	0.557	2.65
hybrid	0.520	10.87	0.585	3.31

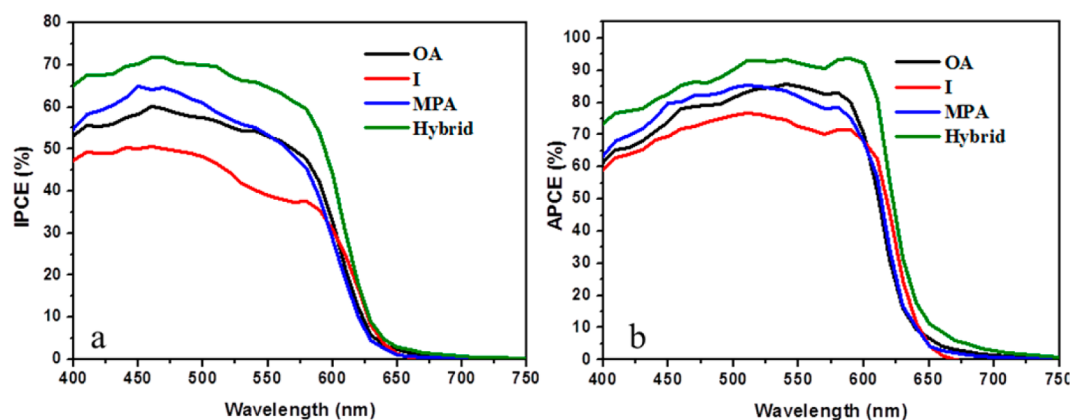


Figure 5. IPCE (a) and APCE (b) curves of QDSCs based on CdSe QDs treated with different surface passivation.

cm^2) and FF value (0.585), together with a desirable V_{oc} (0.52 V). On the other hand, ligand exchange with only MPA just slightly increased the J_{sc} of the solar cells, whereas those cells assembled with only the iodide atom passivated CdSe QDs showed a lower J_{sc} . The V_{oc} of these three kinds of CdSe-QDSCs without hybrid passivation show rather little difference.

The variation in J_{sc} can also be demonstrated by the incident-photon-to-carrier efficiency (IPCE), which is usually used to better understand the nature of sensitizers in QDSCs. Figure 5a shows the IPCE spectra of QDSCs employing different passivated CdSe QDs. The overall photocurrent response parallels the absorption profile of the CdSe QDs sensitized TiO_2 electrodes, but with a little bit broader range (the onset of the IPCE spectra is around 625 nm, whereas the absorption spectra onset is 600 nm), which might arise from light-scattering effect by the large-sized TiO_2 nanoparticles in the TiO_2 electrodes.^{24,25} The IPCE spectra indicate that the hybrid passivated-CdSe QDs based QDSCs show the highest IPCE value (~70%) in the whole response range, followed by the MPA passivated CdSe-QDSCs, the IPCE value of which is slightly higher than that of native OA capped CdSe-QDSCs. The atomic passivated CdSe QDs leads to the lowest IPCE value, in agreement with the lowest J_{sc} in $J-V$ characterization. The calculated J_{sc} from IPCE spectra for the case of hybrid passivation is 9.02 mA/cm^2 , which is close to the measured J_{sc} value in $J-V$ characterization (10.87 mA/cm^2).

The IPCE of the QDSCs is determined by the light harvesting efficiency of the sensitizer (LHE), the quantum yield of the charge injection (ϕ_{inj}) and the collection efficiency at the back contact (η_{cc}): $\text{IPCE} = \text{LHE} \times \phi_{inj} \times \eta_{cc}$. Because of that different LHEs result from different loading amount of the passivated QDs on the TiO_2 electrodes, the IPCE cannot effectively reflect the electron transfer efficiency in the devices. To examine the influence of different passivation on the electron injection and collection from the QDs, the absorbed photon-to-electron conversion efficiency (APCE) was calculated from dividing IPCE by LHE:

$$\text{APCE}(\lambda) = \phi_{inj} \times \eta_{cc} = \frac{\text{IPCE}(\lambda)}{\text{LHE}(\lambda)} = \frac{\text{IPCE}(\lambda)}{1 - 10^{-\text{Abs}(\lambda)}}$$

The result is shown in Figure 5b. After the effect of varied absorbance of different electrodes is ruled out, the APCE value of the hybrid passivated CdSe QDs based solar cells remained the highest. Considering the fact that the electron injection and recombination process can be significantly influenced by the surface states,^{34,35} the higher APCE in the case of hybrid

passivation may relate to fewer surface states, which might be attributed to a reduced number of surface traps after the CdSe QDs being hybrid passivated. The APCE value of the MPA capped CdSe-QDSCs is similar to that of the OA capped CdSe-QDSCs, indicating that the electron transfer efficiency was not degraded after ligand exchange with MPA. Using only atomic passivation gives the lowest APCE of our tested solar cells, and the reason might be the partial aggregation of the iodide passivated CdSe QDs, which may lower the charge injection efficiency from the atomic passivated QDs to TiO_2 nanoparticles.

In addition to the improved J_{sc} after hybrid passivation, a significant enhancement of the fill factor value in the solar cells based on different kinds of passivated CdSe QDs can be observed from Table 1, contributing to gradually increased conversion efficiency of the cells (from 2.34% to 3.31%, step by step). Compared with the use of the native ligand, the FF values of the iodide anion and MPA passivated CdSe QDs based solar cells are much higher (0.535 and 0.557, respectively), and the solar cells based on hybrid passivated CdSe QDs show the highest FF value of 0.585, which is almost 20% higher than that of the OA-CdSe QDSCs. The increase in the FF value after passivation has also been reported in other work; when colloidal PbS QDs are treated with halide anions in solution for colloidal quantum dots photovoltaics,²⁷ or treated after being deposited on TiO_2 electrodes for QDSCs,³⁶ noticeably higher FF values are detected; when CdSe QDs sensitized TiO_2 films are passivated with different kinds of organic and inorganic ligands, a dramatic improvement of the FF also can be observed.^{37–39}

It is commonly postulated that the recombination pathway plays a major role in the fill factor value of QDSCs, and that the shapes of the $J-V$ curves depend on a combination of factors that can be derived from impedance spectroscopy (IS) parameters.^{16,40} Zhitomirsky et al. claimed that by reducing the trap density of QDs and decreasing the recombination centers, the diffusion length will be improved and so a notably higher fill factor can be obtained.⁷ Following this claim, we performed IS characterization under dark conditions to analyze the recombination resistance of the devices. From Figure 6, we can see that the recombination resistance of solar cells based on native ligand OA capped CdSe QDs is the smallest, which means that recombination can easily occur in the device, resulting in the lowest FF value. The recombination resistance of the device modified with iodide anions is larger, so the recombination is suppressed to some extent, which may

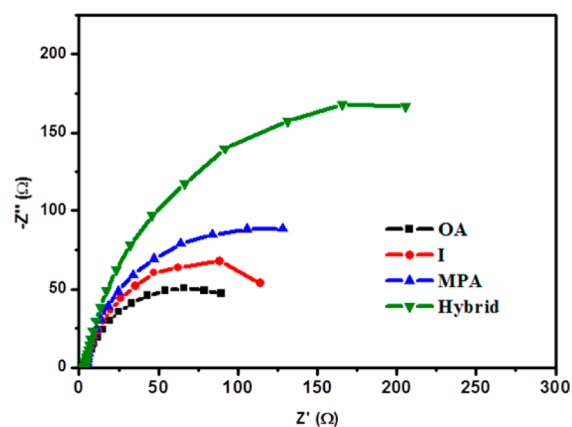


Figure 6. Nyquist plots from IS characterization of QDSCs based on CdSe QDs treated with different surface passivation under dark conditions at -0.53 V forward bias.

indicate that iodine atoms can reduce the surface trap density of QDs, leading to a higher FF value. When CdSe QDs were ligand exchanged by MPA, the recombination resistance of the cells further increased, and an even higher FF value was observed. Though many works have pointed out that MPA may create traps on the surface of QDs,^{41–43} which may induce serious recombination in the solar cells and degrade the efficiency, there are, in our opinion, two main advantages for MPA as ligand for QDs in solar cells. First, QDs become water-soluble after being capped by MPA, and the small size and high wettability of the ligand facilitate sulfide ions in aqueous electrolyte solution to get access to the surface of the QDs, benefiting the hole transfer from the photoexcited QDs to the electrolyte. This is very important for boosting the overall photon conversion efficiency in the QDSCs.⁴⁴ Second, the thiol group of MPA has been reported to be able to extract holes from the photoexcited QDs to the surface ligand,^{45,46} which favors the regeneration and stabilization of the sensitizers.³² Consequently, MPA as capping ligand for QDs can promote the hole extraction from the QDs and reduce the likelihood of charge recombination in the device. Several previous works have achieved impressive performance of QDSCs by using MPA as a ligand,^{9,20,24,25,32} both for high efficiency and long-term stability. When hybrid passivation was carried out to the CdSe QDs, the surface of the QDs was not only capped by MPA, facilitating the hole transfer, but the small iodide anions can also bind to the sites that are inaccessible for a larger MPA molecule, due to the steric hindrance, thus modifying the surface state by forming a more compact ligand layer.²⁹ Therefore, hybrid passivated CdSe QDSCs exhibit the largest recombination resistance and the highest FF value, making the efficiency enhanced by 41% compared to that for native OA capped CdSe QDSCs.

Influence of TBAI Amount. To further explore the effect of iodine atoms in hybrid passivation of CdSe QDs, different amounts of TBAI were added to MPA solution when carrying out the ligand exchange reaction. From Figure 7 and Table 2, we can see that when hybrid ligand solution contained 3 mg of TBAI, the FF value of the corresponding solar cells increased from 0.557 to 0.587, and the V_{oc} was raised by 20 mV, although the current density just shows a little enhancement. This suggests that the recombination of carriers in the devices was effectively suppressed by introducing iodine atoms to the surface of the QDs, and that even a low degree of atom

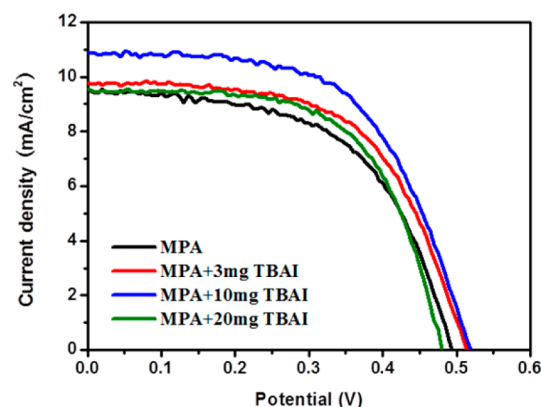


Figure 7. J – V curves of QDSCs based on hybrid passivation with different amount of TBAI.

Table 2. Photovoltaic Parameters of QDSCs Based on Hybrid Passivation with Different Amounts of TBAI

passivant	V_{oc} (V)	J_{sc} (mA/cm ²)	FF	η (%)
MPA	0.495	9.60	0.557	2.65
MPA+3 mg TBAI	0.515	9.80	0.587	2.96
MPA+10 mg TBAI	0.520	10.87	0.585	3.31
MPA+20 mg TBAI	0.480	9.56	0.613	2.81

passivation can lead to a significant beneficial impact. When the amount of TBAI was increased to 10 mg, the J_{sc} increased to 10.87 mA/cm², and the FF value and V_{oc} maintained similar values with that of the solar cell with 3 mg, thereby giving a much higher overall conversion efficiency. When the amount of TBAI further increased to 20 mg, the FF value further grew to 0.613, while both of V_{oc} and J_{sc} showed drastic diminution. The reason for this variation could be that too much TBAI in the ligand solution interferes with the ability of MPA to bind to the CdSe QDs, and so decreases the amount of MPA molecules on the hybrid passivated QDs, which is unfavorable for the adsorption of the QDs onto the TiO₂ photoanodes. As shown in Figure 8, the absorbance of hybrid passivated photoelectrode by 20 mg of TBAI and MPA is lower than that by 10 mg of TBAI and MPA, which degraded the light harvesting efficiency and the J_{sc} of the solar cells. Consequently, a suitable amount of TBAI is of great importance for the hybrid passivation of QDs when applied to QDSCs.

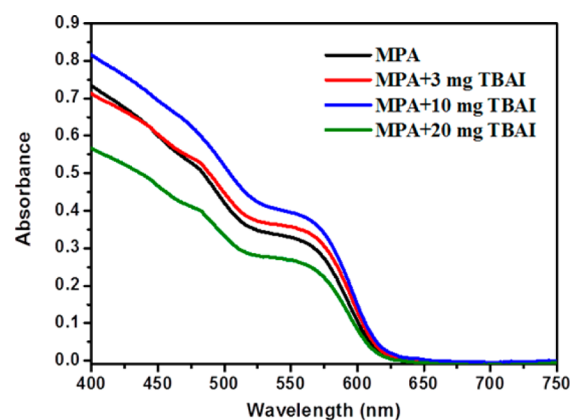


Figure 8. UV–vis absorption spectra of hybrid passivated CdSe QDs-sensitized TiO₂ electrodes with different amount of TBAI.

CONCLUSIONS

In this work, we improved the efficiency of CdSe quantum dot-sensitized solar cells (QDSCs) by hybrid passivation of CdSe QDs with mercaptopropionic acid (MPA) and iodide anions using a solution process. Our study shows that the loading efficiency of the CdSe QDs on TiO₂ electrodes can indeed be increased by employing MPA for ligand capping of the QDs, which also promotes hole transfer from the sensitizer to the electrolyte. The complementary binding with iodide anions can furthermore reduce the surface traps on the QDs and increase the recombination resistance in the devices, resulting in higher J_{sc} value and a boost of the FF value. Though only MPA passivation can increase the coverage of QDs and enlarge the recombination resistance, it is not as effective as hybrid passivation to enhance the efficiency of solar cells due to some incurable surface defects on the MPA capped-QDs. Using only atomic passivation is unfavorable for the deposition of QDs, though it still can remedy part of the surface traps on the QDs. Therefore, through collaborating with MPA and iodide anions, the hybrid passivation make the QDSCs exhibit the best photovoltaic performance. Moreover, the choice of the amount of TBAI is found to be crucial for an optimal effect of hybrid passivation, as an excess of iodide anions in the ligand solution could interfere with the binding of MPA to the surface of the QDs. This work demonstrates a new strategy to enhance QDSC performance by employing different kinds of functional ligands at the same time, as hybrid passivation, to the QDs. In further investigations, we will focus on applying this hybrid passivation strategy to nontoxic CuInS₂ based QDs, which is very important for large-scale applications of QDSCs.

ASSOCIATED CONTENT

Supporting Information

XRD pattern of as-synthesized QDs, FTIR spectra and TEM images of colloidal CdSe QDs treated with different passivation and statistic analysis of the photovoltaic parameters of QDSCs based on CdSe QDs treated with different surface passivation. This material is available free of charge via the Internet at <http://pubs.acs.org>.

AUTHOR INFORMATION

Corresponding Authors

*L. Sun. E-mail: lichengs@kth.se. Fax: (+46) 8-791-2333.

*H. Ågren. E-mail: agren@theochem.kth.se. Fax: +46 8 55378416.

Notes

The authors declare no competing financial interest.

ACKNOWLEDGMENTS

This work was financially supported by the Swedish Research Council, the Swedish Energy Agency, the Knut and Alice Wallenberg Foundation and the China Scholarship Council (CSC). We thank Dr. Xin Li (KTH), Jiajia Gao (KTH) and Lei Wang (KTH) for their helpful discussion and advices. We also specially thank Na Kong (KTH) for her great help with FTIR measurements.

REFERENCES

(1) Kamat, P. V.; Tvrđy, K.; Baker, D. R.; Radich, J. G. Beyond Photovoltaics: Semiconductor Nanoarchitectures for Liquid-Junction Solar Cells. *Chem. Rev.* **2010**, *110*, 6664–6688.

(2) Mora-Seró, I.; Bisquert, J. Breakthroughs in the Development of Semiconductor-Sensitized Solar Cells. *J. Phys. Chem. Lett.* **2010**, *1*, 3046–3052.

(3) Nozik, A. J.; Beard, M. C.; Luther, J. M.; Law, M.; Ellingson, R. J.; Johnson, J. C. Semiconductor Quantum Dots and Quantum Dot Arrays and Applications of Multiple Exciton Generation to Third-Generation Photovoltaic Solar Cells. *Chem. Rev.* **2010**, *110*, 6873–6890.

(4) Rühle, S.; Shalom, M.; Zaban, A. Quantum-Dot-Sensitized Solar Cells. *ChemPhysChem* **2010**, *11*, 2290–2304.

(5) Yang, Z.; Chen, C.-Y.; Roy, P.; Chang, H.-T. Quantum Dot-Sensitized Solar Cells Incorporating Nanomaterials. *Chem. Commun.* **2011**, *47*, 9561–9571.

(6) Chen, G.; Seo, J.; Yang, C.; Prasad, P. N. Nanochemistry and Nanomaterials for Photovoltaics. *Chem. Soc. Rev.* **2013**, *42*, 8304–8338.

(7) Zhitomirsky, D.; Voznyy, O.; Levina, L.; Hoogland, S.; Kemp, K. W.; Ip, A. H.; Thon, S. M.; Sargent, E. H. Engineering Colloidal Quantum Dot Solids within and beyond the Mobility-Invariant Regime. *Nat. Commun.* **2014**, *5*, 3803.

(8) Chuang, C.-H. M.; Brown, P. R.; Bulović, V.; Bawendi, M. G. Improved Performance and Stability in Quantum Dot Solar Cells through Band Alignment Engineering. *Nat. Mater.* **2014**, *13*, 796–801.

(9) Wang, J.; Mora-Seró, I.; Pan, Z.; Zhao, K.; Zhang, H.; Feng, Y.; Yang, G.; Zhong, X.; Bisquert, J. Core/Shell Colloidal Quantum Dot Exciplex States for the Development of Highly Efficient Quantum-Dot-Sensitized Solar Cells. *J. Am. Chem. Soc.* **2013**, *135*, 15913–15922.

(10) Radich, J. G.; Peeples, N. R.; Santra, P. K.; Kamat, P. V. Charge Transfer Mediation Through Cu_xS. The Hole Story of CdSe in Polysulfide. *J. Phys. Chem. C* **2014**, *118*, 16463–16471.

(11) Pan, Z.; Mora-Seró, I.; Shen, Q.; Zhang, H.; Li, Y.; Zhao, K.; Wang, J.; Zhong, X.; Bisquert, J. High-Efficiency “Green” Quantum Dot Solar Cells. *J. Am. Chem. Soc.* **2014**, *136*, 9203–9210.

(12) Kamat, P. V. Quantum Dot Solar Cells. The Next Big Thing in Photovoltaics. *J. Phys. Chem. Lett.* **2013**, *4*, 908–918.

(13) Hanna, M. C.; Nozik, A. J. Solar Conversion Efficiency of Photovoltaic and Photoelectrolysis Cells with Carrier Multiplication Absorbers. *J. Appl. Phys.* **2006**, *100*, 074510.

(14) Semonin, O. E.; Luther, J. M.; Choi, S.; Chen, H.-Y.; Gao, J.; Nozik, A. J.; Beard, M. C. Peak External Photocurrent Quantum Efficiency Exceeding 100% via MEG in a Quantum Dot Solar Cell. *Science* **2011**, *334*, 1530–1533.

(15) Stolle, C. J.; Harvey, T. B.; Pernik, D. R.; Hibbert, J. I.; Du, J.; Rhee, D. J.; Akhavan, V. A.; Schaller, R. D.; Korgel, B. A. Multiexciton Solar Cells of CuInSe₂ Nanocrystals. *J. Phys. Chem. Lett.* **2013**, *5*, 304–309.

(16) Mora-Seró, I.; Giménez, S.; Fabregat-Santiago, F.; Gómez, R.; Shen, Q.; Toyoda, T.; Bisquert, J. Recombination in Quantum Dot Sensitized Solar Cells. *Acc. Chem. Res.* **2009**, *42*, 1848–1857.

(17) Lee, J.-W.; Son, D.-Y.; Ahn, T. K.; Shin, H.-W.; Kim, I. Y.; Hwang, S.-J.; Ko, M. J.; Sul, S.; Han, H.; Park, N.-G. Quantum-Dot-Sensitized Solar Cell with Unprecedentedly High Photocurrent. *Sci. Rep.* **2013**, *3*, 1050.

(18) McDaniel, H.; Fuke, N.; Makarov, N. S.; Pietryga, J. M.; Klimov, V. I. An Integrated Approach to Realizing High-Performance Liquid-Junction Quantum Dot Sensitized Solar Cells. *Nat. Commun.* **2013**, *4*, 2887.

(19) He, G. S.; Tan, L.-S.; Zheng, Q.; Prasad, P. N. Multiphoton Absorbing Materials: Molecular Designs, Characterizations, and Applications. *Chem. Rev.* **2008**, *108*, 1245–1330.

(20) Zhang, H.; Cheng, K.; Hou, Y. M.; Fang, Z.; Pan, Z. X.; Wu, W. J.; Hua, J. L.; Zhong, X. Efficient CdSe Quantum Dot-Sensitized Solar Cells Prepared by a Postsynthesis Assembly Approach. *Chem. Commun.* **2012**, *48*, 11235–11237.

(21) Choi, Y.; Seol, M.; Kim, W.; Yong, K. Chemical Bath Deposition of Stoichiometric CdSe Quantum Dots for Efficient Quantum-Dot-Sensitized Solar Cell Application. *J. Phys. Chem. C* **2014**, *118*, 5664–5670.

- (22) Dollefeld, H.; Hoppe, K.; Kolny, J.; Schilling, K.; Weller, H.; Eychmuller, A. Investigations on the Stability of Thiol Stabilized Semiconductor Nanoparticles. *Phys. Chem. Chem. Phys.* **2002**, *4*, 4747–4753.
- (23) Kumar, R.; Roy, I.; Ohulchanskyy, T. Y.; Goswami, L. N.; Bonoiu, A. C.; Bergey, E. J.; Trampusch, K. M.; Maitra, A.; Prasad, P. N. Covalently Dye-Linked, Surface-Controlled, and Bioconjugated Organically Modified Silica Nanoparticles as Targeted Probes for Optical Imaging. *ACS Nano* **2008**, *2*, 449–456.
- (24) Pan, Z.; Zhao, K.; Wang, J.; Zhang, H.; Feng, Y.; Zhong, X. Near Infrared Absorption of CdSe_xTe_{1-x} Alloyed Quantum Dot Sensitized Solar Cells with More than 6% Efficiency and High Stability. *ACS Nano* **2013**, *7*, S215–S222.
- (25) Pan, Z.; Zhang, H.; Cheng, K.; Hou, Y.; Hua, J.; Zhong, X. Highly Inverted Type-I CdS/CdSe Core/Shell Structure QD-Sensitized Solar Cells. *ACS Nano* **2012**, *6*, 3982–3991.
- (26) Tang, J.; Kemp, K. W.; Hoogland, S.; Jeong, K. S.; Liu, H.; Levina, L.; Furukawa, M.; Wang, X.; Debnath, R.; Cha, D.; Chou, K. W.; Fischer, A.; Amassian, A.; Asbury, J. B.; Sargent, E. H. Colloidal-Quantum-Dot Photovoltaics Using Atomic-Ligand Passivation. *Nat. Mater.* **2011**, *10*, 765–771.
- (27) Ning, Z.; Ren, Y.; Hoogland, S.; Voznyy, O.; Levina, L.; Stadler, P.; Lan, X.; Zhitomirsky, D.; Sargent, E. H. All-Inorganic Colloidal Quantum Dot Photovoltaics Employing Solution-Phase Halide Passivation. *Adv. Mater.* **2012**, *24*, 6295–6299.
- (28) Thon, S. M.; Ip, A. H.; Voznyy, O.; Levina, L.; Kemp, K. W.; Carey, G. H.; Masala, S.; Sargent, E. H. Role of Bond Adaptability in the Passivation of Colloidal Quantum Dot Solids. *ACS Nano* **2013**, *7*, 7680–7688.
- (29) Ip, A. H.; Thon, S. M.; Hoogland, S.; Voznyy, O.; Zhitomirsky, D.; Debnath, R.; Levina, L.; Rollny, L. R.; Carey, G. H.; Fischer, A.; Kemp, K. W.; Kramer, I. J.; Ning, Z.; Labelle, A. J.; Chou, K. W.; Amassian, A.; Sargent, E. H. Hybrid Passivated Colloidal Quantum Dot Solids. *Nat. Nanotechnol.* **2012**, *7*, 577–582.
- (30) Liao, L.; Zhang, H.; Zhong, X. Facile Synthesis of Red- to Near-Infrared-Emitting CdTe_xSe_{1-x} Alloyed Quantum Dots via a Non-injection One-Pot Route. *J. Lumin.* **2011**, *131*, 322–327.
- (31) Anderson, N. C.; Owen, J. S. Soluble, Chloride-Terminated CdSe Nanocrystals: Ligand Exchange Monitored by ¹H and ³¹P NMR Spectroscopy. *Chem. Mater.* **2012**, *25*, 69–76.
- (32) Sambur, J. B.; Riha, S. C.; Choi, D.; Parkinson, B. A. Influence of Surface Chemistry on the Binding and Electronic Coupling of CdSe Quantum Dots to Single Crystal TiO₂ Surfaces. *Langmuir* **2010**, *26*, 4839–4847.
- (33) Kongkanand, A.; Tvrđy, K.; Takechi, K.; Kuno, M.; Kamat, P. V. Quantum Dot Solar Cells. Tuning Photoresponse through Size and Shape Control of CdSe–TiO₂ Architecture. *J. Am. Chem. Soc.* **2008**, *130*, 4007–4015.
- (34) Hetsch, F.; Xu, X.; Wang, H.; Kershaw, S. V.; Rogach, A. L. Semiconductor Nanocrystal Quantum Dots as Solar Cell Components and Photosensitizers: Material, Charge Transfer, and Separation Aspects of Some Device Topologies. *J. Phys. Chem. Lett.* **2011**, *2*, 1879–1887.
- (35) Zhang, J. Z. Ultrafast Studies of Electron Dynamics in Semiconductor and Metal Colloidal Nanoparticles: Effects of Size and Surface. *Acc. Chem. Res.* **1997**, *30*, 423–429.
- (36) Niu, G.; Wang, L.; Gao, R.; Ma, B.; Dong, H.; Qiu, Y. Inorganic Iodide Ligands in Ex Situ PbS Quantum Dot Sensitized Solar Cells with I⁻/I³⁻ Electrolytes. *J. Mater. Chem.* **2012**, *22*, 16914–16919.
- (37) De la Fuente, M. S.; Sánchez, R. S.; González-Pedro, V.; Boix, P. P.; Mhaisalkar, S. G.; Rincón, M. E.; Bisquert, J.; Mora-Seró, I. Effect of Organic and Inorganic Passivation in Quantum-Dot-Sensitized Solar Cells. *J. Phys. Chem. Lett.* **2013**, *4*, 1519–1525.
- (38) Liu, F.; Zhu, J.; Wei, J.; Li, Y.; Hu, L.; Huang, Y.; Takuya, O.; Shen, Q.; Toyoda, T.; Zhang, B.; Yao, J.; Dai, S. Ex Situ CdSe Quantum Dot-Sensitized Solar Cells Employing Inorganic Ligand Exchange To Boost Efficiency. *J. Phys. Chem. C* **2013**, *118*, 214–222.
- (39) Yun, H. J.; Paik, T.; Edley, M. E.; Baxter, J. B.; Murray, C. B. Enhanced Charge Transfer Kinetics of CdSe Quantum Dot-Sensitized Solar Cell by Inorganic Ligand Exchange Treatments. *ACS Appl. Mater. Interfaces* **2014**, *6*, 3721–3728.
- (40) Fabregat-Santiago, F.; Garcia-Belmonte, G.; Mora-Sero, I.; Bisquert, J. Characterization of Nanostructured Hybrid and Organic Solar Cells by Impedance Spectroscopy. *Phys. Chem. Chem. Phys.* **2011**, *13*, 9083–9118.
- (41) Baker, D. R.; Kamat, P. V. Tuning the Emission of CdSe Quantum Dots by Controlled Trap Enhancement. *Langmuir* **2010**, *26*, 11272–11276.
- (42) Hines, D. A.; Kamat, P. V. Quantum Dot Surface Chemistry: Ligand Effects and Electron Transfer Reactions. *J. Phys. Chem. C* **2013**, *117*, 14418–14426.
- (43) Guijarro, N. S.; Shen, Q.; Giménez, S.; Mora-Seró, I. n.; Bisquert, J.; Lana-Villarreal, T.; Toyoda, T.; Gómez, R. Direct Correlation between Ultrafast Injection and Photoanode Performance in Quantum Dot Sensitized Solar Cells. *J. Phys. Chem. C* **2010**, *114*, 22352–22360.
- (44) Kamat, P. V.; Christians, J. A.; Radich, J. G. Quantum Dot Solar Cells: Hole Transfer as a Limiting Factor in Boosting the Photoconversion Efficiency. *Langmuir* **2014**, *30*, 5716–5725.
- (45) Bullen, C.; Mulvaney, P. The Effects of Chemisorption on the Luminescence of CdSe Quantum Dots. *Langmuir* **2006**, *22*, 3007–3013.
- (46) Tan, Y.; Jin, S.; Hamers, R. J. Influence of Hole-Sequestering Ligands on the Photostability of CdSe Quantum Dots. *J. Phys. Chem. C* **2012**, *117*, 313–320.